Tahir_2019_Mater._Res._Express_6_035705.pdf

by

Submission date: 26-May-2023 12:30PM (UTC+0700)
Submission ID: 2102213588
File name: Tahir_2019_Mater._Res._Express_6_035705.pdf (1.18M)
Word count: 5892
Character count: 28040

Materials Research Express

PAPER

Modification in electronic, structural, and magnetic properties based on composition of composites Copper (II) Oxide (CuO) and Carbonaceous material

IOP Publishing Mater. Res. Express 6 (2019) 035705 https://doi.org/10.1088/2053-1591/aaf7da

Materials Research Express

PAPER

Modification in electronic, structural, and magnetic properties based on composition of composites Copper (II) Oxide (CuO) and Carbonaceous material

RECEIVED
8 November 2018
REVISED
4 December 2018
ACCEPTED FOR PUBLICATION
11 December 2018
PUBLISHED
21 December 2018

Dahlang Tahir[1], Sultan Ilyas[1], Bualkar Abdullah[1], Bidayatul Armynah[1], Kyousik Kim[2] and Hee Jae Kang[2]
[1] Department of Physics, Hasanuddin University, Makassar 90245, Indonesia
[2] Department of Physics, Chungbuk National University, Cheongju, 28644, Republic of Korea
E-mail: dtahir@fmipa.unhas.ac.id

Keywords: composites CuO-AC, REELS, XPS, FTIR, XRD, electronic properties

Abstract

Modification in electronic properties of composite copper (II) oxide (CuO) and activated carbon (AC) were obtained by using x-ray photoelectron spectroscopy (XPS), reflection electron energy loss spectroscopy (REELS), and Fourier transforms infrared spectroscopy (FTIR), structural properties by x-ray diffraction (XRD), and magnetic properties by vibrating sample magnetometer (VSM). The bandgap values of composite are 2.1 eV, 2.4 eV, 2.8 eV, and 3.1 eV for 10% AC, 15% AC, 20% AC, and 25% AC, respectively. XPS results showed that the pore of AC effectively increase the stable bonding due to the present strong bonding of O–C–Cu_{1-x}–O in the composites which is effectively for increasing efficiency in devices applications. It should be leading to significant modification in the electronic and the structural properties of composites CuO–AC by increasing the amount of AC as organic linker in the composites. The pore and the concentration of AC as organic linker play an important role in the increasing magnetic and the reflection loss properties which is high stability for absorber applications.

1. Introduction

Copper metals and their oxides are materials widely used as a conductor in metallization of modern microelectronic devices due to the specific electrical, structural, catalytic, optical and magnetic properties [1–3]. Ionic states produced from the interaction between the surface of copper with different oxidation state which can be monovalent (Cu^{+}) formed CuO (cupric oxide) or divalent (Cu^{2+}) formed Cu_2O (cuprous oxide) [2–4]. The CuO combined with carbonaceous materials in the form of composite become interesting materials for various applications due to the environmental viability and low density for heterogeneous catalysts, pharmaceutical, biomedical, cosmetic formulations, and absorber materials of electromagnetics (EM) waves [1–8].

Chemical stability of organic linker (chemical bonding) between carbonaceous materials in contact with metal oxide is intensively studied for increasing efficiency in devices applications [2, 4, 7]. The chemical bonding is high complexes at the surface and relatively easy for breaking during the operation of the devices applications as reported in [9, 10] by using polymers as a linker. The carbonaceous (AC) material is usually large internal surface areas and pore volumes, which can be used to help for reducing the formation of unstable bonding at the surface of composites [11]. For considering the bonding stability, it is important to understand the electronic properties, the structural properties, and bonding formation between AC atom and metal oxide atom [4, 5, 7, 12, 13].

Hence, the bonding formation, electronic properties, structural properties, and magnetic properties are the most fundamental properties needed in characterizing because these properties influence to the performance in device applications. The bonding formation and electronic properties of composite copper oxide and AC can be determined by REELS by considering the bandgap and the interband transition, for XPS by considering the core

level spectra of Cu 2p, O 1s, C 1s, and O-KLL spectra. XPS and REELS spectroscopy are surface sensitive and they are capable of characterizing the electronic properties of materials (thin films and powder) because the low energy-loss region reflects to the structure of the valence and conduction electrons [7, 14–22]. The primary electron energy of REELS used for determining the bandgap usually at 1.5 keV for excitation with about 0.8 eV full width at half maximum (FWHM) of the elastic peak. For inelastic peak is representing energy loss which was indicated the interference between surface and bulk loss processes when the moving electron leaves the surface. The validity of electronic properties from XPS for REELS [14–27] has been extensively and successfully used to obtain the electronic properties of polymers, compound metals, ultrathin dielectrics, semiconductors, transparent oxide films, and composites [7, 14–28].

The chemical bonding state between CuO and AC is essential to understand in the modification electronic properties which can be producing the stable bonding organic-inorganic metal oxide for various applications. So far, bonding formation, electronic properties, structural properties, and magnetic properties of CuO–AC composites have not been experimentally investigated adequately. The bonding formation and electronic properties of CuO–AC composites were investigated by using x-ray photoelectron spectroscopy (XPS), Fourier transform infra-red spectroscopy (FTIR), and reflection electron energy loss spectroscopy (REELS). The magnetic properties were investigated by using vibrating sample magnetometer (VSM), structural properties by x-ray diffraction (XRD), and absorption characteristic by vector network analyzer (VNA) measurements.

2. Materials and methods

Copper (II) oxide powder (CuO) supplied from Merck with particle size is $<10\ \mu$m and assay 98%. Activated carbon (AC) supplied from the local company PT. Cahaya Indo Abadi Indonesia with purity >95%, average diameter <:10 μm, and surface area: >240 m g^{-1}. PVA (Polyvinyl Alcohol) from Merck with purity 99.5%.

The experimental procedure and characterization system in the present study was described in detail in [7] and briefly repeated here. We crushed and sieved with 200 meshes of the activated carbon (AC) into powder by using a mortar. We mixed CuO with AC by Retsch MM for 30 min at frequency 10 Hz. We have 2 samples for every composition, the first sample used to determine the time of homogenous mixed composite which was monitored by x-ray fluorescence (XRF) and the second sample used for characterization by mixed directly (30 min) based on the desired time from the first sample. It's about 15 gram of the final mass for each sample in composite which is consists of 10%, 15%, 20%, and 25% of AC.

By using the VG ESCALAB 210, the XPS and the REELS spectra were obtained with the constant analyzer pass energy of 20 eV and Mg $K\alpha$ as x-ray source which was reported in our previous paper [8, 12–15, 16–25] in detail. The incident angles of electrons were 55° and take off angles is 0° from the surface normal. REELS were measured with the primary electron energy of 1.5 keV for excitation and about 0.8 eV for the full width at half maximum (FWHM) of the elastic peak.

X-ray Diffraction (XRD) spectra were collected on XRD spectroscopy (Shimadzu 7000) with Cu $K\alpha$ radiation ($\lambda = 1.5405$ Å) over the angular range $10° \leqslant 2\theta \leqslant 80°$, operating at 30 kV and 10 mA. The quantitative analysis of XRD spectra was used to determine the crystallite size, lattice strain, lattice parameter and porosity of the CuO, AC, and composites CuO–AC [29].

Fourier Transforms Infrared (FTIR) spectroscopy spectra were collected from FT-IR spectrometer (Shimadzu Corp) type IRPrestige-21 with deuterated triglycine sulfate doped with L-alanine (DLATGS) detector, bright ceramic light source, and KBr beamsplitter. All FTIR spectra were collected over the range of 4000–600 cm^{-1} and 16 co-added scans in Transmittance units. The magnetic studies were performed from Oxford Instruments with vibrating sample magnetometer (VSM) 1.2 H type.

To obtain the samples pellet for electromagnetic wave absorber performance powder composites were added with 2% PVA about 5 ml for each composition of the samples and then stirred at 50 °C for 30 min to obtain slurry form. The slurry form was pouring in to the mold and then pressing by using hydraulic compactor at a pressure of 50 kPa for various thicknesses (2 mm, 3 mm, and 4 mm) then it was cooled naturally for 5–7 min. The pellets samples were annealed in Muffle furnace (Daihan Labtech Co., LTD) for 5 h at 80 °C. The electromagnetic wave absorber performance was measured by using Vector Network Analyzer (VNA) at the frequency ranges from 2.5 GHz to 8 GHz (Rohde and Schwarz ZVHB).

3. Results and discussion

Figure 1 show REELS and XPS full spectra for AC, CuO, and composites CuO–AC.

The XPS full spectra shown in figure 1 have a distinct and clear sharp-peak structure CuO which was recognized as Cu 3s, O 1s, Cu LMM, Cu 2p, and O KLL, and for AC, the highest peak is C1s followed by O 1s, C KLL and O KLL [2, 4, 13, 17]. The presence of C 1s and C KLL core-level for CuO is due to the neutral carbon

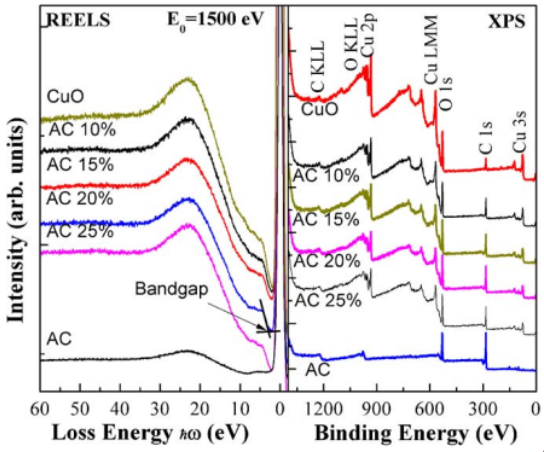

Figure 1. Electron spectroscopy spectra for CuO and composit O–AC (10%, 15%, 20%, and 25% AC). (a) Reflection electron energy loss (REELS) spectra at the primary energy 1500 eV. (b) X-ray photoelectron spectroscopy (XPS) full spectra.

onto the surface of the sample, therefore the carbon peak intensity is weak but for composite intensity increase significantly with increasing the amount of AC. For composite, the peaks of core level obtained from CuO and AC increase with increasing the amount of the base material indicated the homogenous of composites, as can be seen in Cu 3s, Cu LMM, Cu 2p from CuO and C 1s and C KLL from AC.

From the REELS spectra, the band gap is determined as the crossing point of maximum negative slope near the edge values with the background level (as can be seen in figure 1 (REELS), the arrow denotes the band gap energy). The detail explanation for determining the band gap from REELS spectra are in our previous paper [7, 14–28]. The band gap value for AC is 4.5 eV as reported in our previous paper [7], CuO is 1.2 eV similar reported in [17] and band gap for composites are increased slightly from 2.1 eV for 10% AC to 3.1 eV for 25% AC which was similar to values reported in [7] for composite Fe_2O_3–AC. For semiconductor materials usually the electronic structure can be identified through the bandgap, which is basically the gap of energy between valence band maximum and conduction band minimum [13, 14, 20]. The valence band maximum is the highest energy position occupied by molecular orbital which also can be determined the ionization potential of the bulk materials from this energy position [13, 14, 20]. The conduction band minimum indicated the lowest position unoccupied molecular orbital which also can be determined the electron affinity of compound [13, 14, 20].

Concentration of carbonaceous particle as organic linker in the composites can be tuned which is an influence to the band gap. The strong bonding formation of composites in this study was confirmed by increasing in the band-gap as concentration of AC increase due to the interfacial charge transfer complex at the surface between hydroxyl groups of CuO and carbonaceous (AC) as reported in [7] for Fe_3O_4–AC. This result indicated the strong bonding of O–C–Cu_{1-x}–O was formed due to the effective orbital hybridization between 3d (Cu) orbital of CuO and the π(C) orbitals of amorphous carbon and also 2p (O) orbital from both of AC and CuO [17].

REELS spectrum for CuO shows peaks at 8, 24, and 58 eV. A peak at 8 eV shows strong peak which is usually identified as surface plasmon as reported in [14] for ZrO_2 at 8 eV and for Fe at ~9 eV [22]. Peak at 24 eV shows broad peak which is similar reported in [7] for Fe_3O_4 and [22] for Fe. For AC, peak at 8 eV is π plasmon or surface plasmon which is typical for polymeric materials as reported in [7]. The broad peak at 24 eV for composites in this study corresponds to the collective excitation of the $\sigma + \pi$ plasmon or bulk plasmon as reported for composite Fe_3O_4–AC in [7] and interband transition from d-band to unoccupied state above E_F as reported in [17] for Cu and [22] for Fe and Pd. For composites with composition of AC up to 25% in composites, the REELS spectrum qualitatively shows the same characteristics with the energy loss of CuO due to the CuO has a strong effect in the composites.

Figure 2 shows the XPS core-level spectra of AC, CuO and composites CuO–AC for Cu 2p (a), O 1s (b), and C 1s (c). The Cu 2p spectra show 2p3/2 core level at 933.53 eV and 2p1/2 core level at 953.83 eV. As can be seen in this study another peaks assigned satellite shake-up at about 8.5 eV and 11.5 eV above and below the main core level of Cu1/2, respectively, which are in best agreement reported in [2, 13]. Satellite shake up for all samples shows strong features indicated no presence of Cu_2O structure (phase) due to the appearance of Cu^{1+} ions as reported in [13]. From the figure 2(a) we can see clearly the spin splitting of Cu 2p decrease with

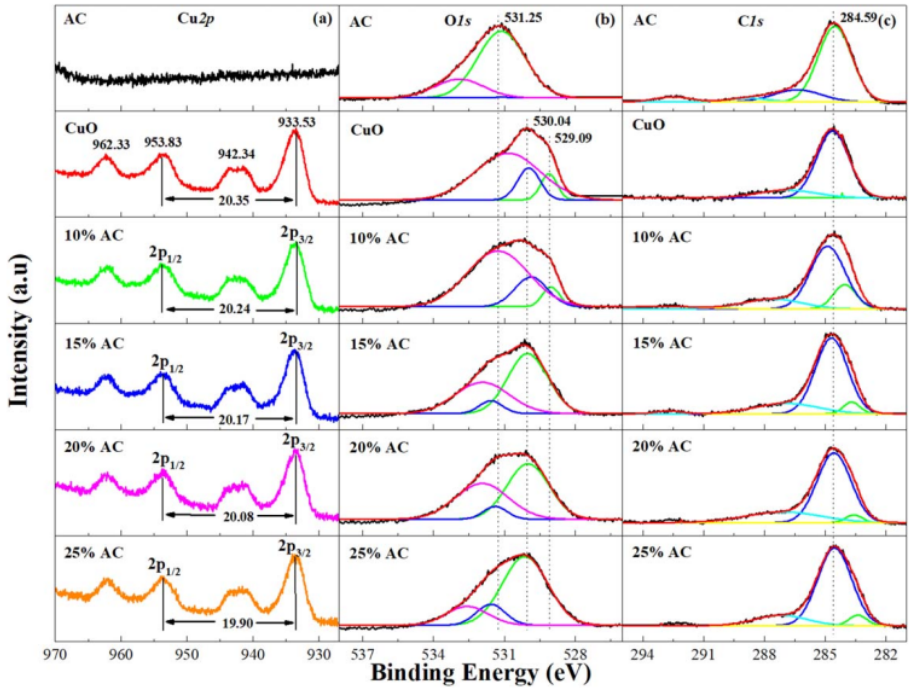

Figure 2. XPS core level photoelectron spectra for CuO and composite CuO–AC (10%, 15%, 20%, and 25% AC). (a) Cu *2p*, (b) O 1s, and (c) C 1s.

increasing the amount of AC in the composites due to the formation of strong bonding by the organic linker between the particle of AC and surface hydroxyl group of CuO as reported in [7]. For composites, the increasing of the amount of AC from 10% to 25 wt % in the composites CuO–AC shows the effective orbital's mixing was formed and the optical band gap energy also increased.

For O 1s in AC shows peaks at 533 eV were assigned C–O and 532 eV could be assigned to the high amount of Si or Fe presence in carbonaceous organic in the form C=O–Si or C=O–Fe. For CuO, three peaks at 532 eV, 530 eV, and 529 eV were assigned to C=O, Cu–O, O–Cu–O, respectively. For composite, interesting to note the position of C=O bond was found, and the intensity increases with increasing the amount of AC in composite. These findings was suggesting the increasing of the existence bonding states of C=Cu due to substitution of oxygen atoms in C=O bonding with Cu atom. The O–Cu–O bonding decreases due to substitution of oxygen atoms with C atom in composites leading to formation of O–C_x–$Cu_{1-x}O$. This result shows significant modification in electronic properties of composites CuO–AC by increasing the amount of AC in the composites. The number of second-nearest neighbor Cu or C atoms strongly affected to the O 1s chemical bonding formation in composites [30–34].

C1s shows three peaks at 284.5 eV, 287.8 eV and 292.5 eV assigned as C=C, C–OH, and OH–C=O, respectively. The small peak at 292.5 eV probably comes from the organic matter of AC, as can be seen in the figure 2(c) peaks more intense with increasing the amount of AC in the compound, similar for peak C–OH. This means that the amount of C=C bond could be responsible in modification of electronic properties of composites CuO–AC. By investigating the chemical bonding of O 1s, C 1s core level spectra by using XPS, the binary deposit formation identified is oxide, denoted as O–C_x–$Cu_{1-x}O$. The composites of CuO–AC formation was confirmed from XPS and REELS spectrum.

Figure 3 shows chemical bonding formation by FT-IR spectroscopy for AC, CuO, and composites CuO–AC. As shown in figure 3, the characteristic peaks of carbonaceous were described in detail in our previous paper [7]. The composites CuO–AC in this study shows small existing peak of C=C cm^{-1} indicated normal stretching and bending vibration of carbonaceous (AC) molecules [4, 13, 30 318], see table 1. However, the peak appeared at the wave number 500–700 cm^{-1} mainly attributed to Cu–O–C bonding. For 10% AC, the small peak nearly 700 cm^{-1} increases with increasing the amount of AC and also shifted to the higher wave number position which attributed to the C–C bonding from AC which was reported in [30] for organic materials. The C–C bond

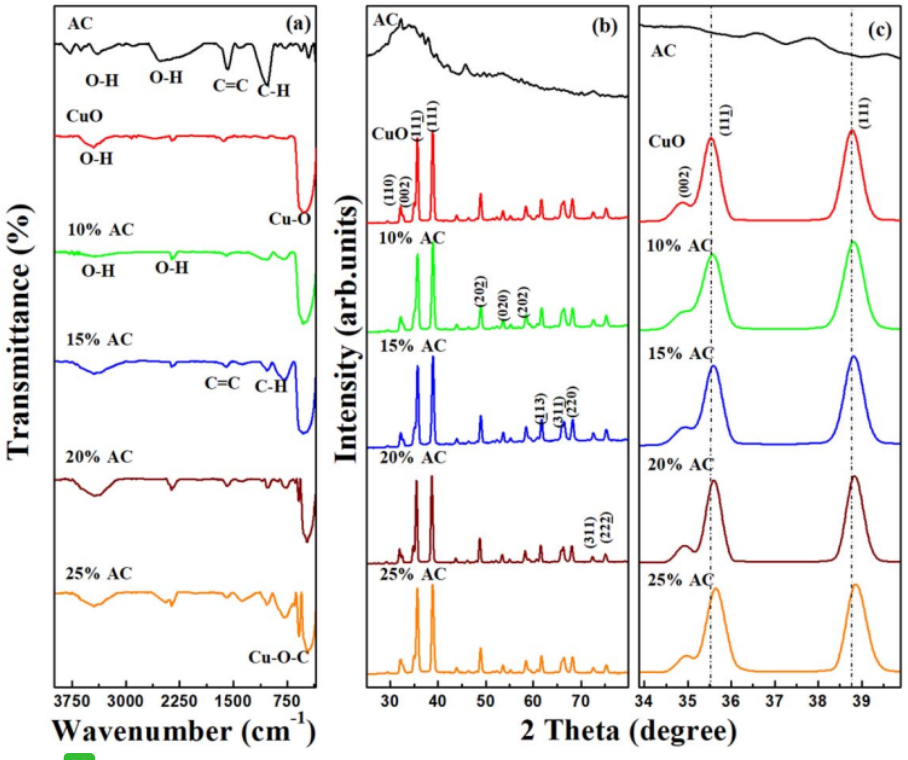

Figure 3. Fourier transform infrared (FTIR) (a), x-ray diffraction (XRD) (b), and zoom XRD for main the peaks (35.62° and 38.85°) (c) spectra for CuO and composite CuO–AC (10%, 15%, 20%, and 25% AC).

Table 1. Type of bonding and vibration mode derived from FTIR spectra in figure 3 (a) for CuO and composite CuO–AC (activated carbon) (10% AC, 15% AC, 20% AC, and 25% AC).

Wavenumber (cm^{-1})				
CuO	AC	CuO Composite (CuO/AC)	Type of bond	Vibrating mode
435–600	—	435–600	Cu–O, Cu–O–C	Inorganic groups
—	950–1250	950–1250	C–H	Aromatic plane bending
—	1538–1558	1538–1558	C=C	Stretching rings
3200–3600	2250–2700	2250–2700	O–H	Aromatic rings carboxylic
	3200–3600	3200–3600		

vibration peak confirms that formation of the carbonaceous structure of composites. The broad main peak for 10% and 15% AC at around 500 cm^{-1} from CuO increases broadening and decrease for >15% AC by introducing the sharp peak which indicated the modification of electronic structures of composite due to the as O–C_x–$Cu_{1-x}O$ binary was formed. From the analysis spectrum of REELS and XPS for composite shows consistent result with FTIR spectra, which is clearly demonstrated the functional pore of AC molecules forming strong and stable bonding between metal oxide and carbonaceous atom. These results were confirmed that the CuO atoms were strongly deposited in the pore of AC [7]. The peaks at 3438 and 2508 cm^{-1} are attributed to the O–H ring vibration and C–O–H bond, respectively. The present study shows the pore of AC effectively increase the stability bonding formation of composites CuO–AC material.

Figure 3(b) shows XRD spectra of CuO and composite CuO–AC and (c) zoom for the main peak (35.62° and 38.85°). The diffraction peaks for CuO are similar with all composites (small shifted to higher angle diffraction for high amount of AC) in this study at 2θ = 32.60°, 34.69°, 35.62°, 38.85°, 48.86°, 53.56°, 58.38°, 61.62°, 65.88°, 66.32°, 68.09°, 72.47°, 75.20° which is shows narrow and intense peaks indicating high crystallinity, best agreement with diffraction peaks reported in [1, 2, 13]. Based on the JCPDS (00-048-1548) data, the CuO and

Table 2. Crystallite size, lattice parameter, and porosity derived from XRD spectra in figure 3(b) for CuO and composite CuO–AC (activated carbon) (10% AC, 15% AC, 20% AC, and 25% AC).

Sample ID	Crystallite size (nm) (D)	lattice parameter (Å)	Volume (V_{cal})	Dislocation density ($1/D^2$) (nm^{-2})	Porosity (%)
CuO	20.81	a = 4.67, b = 3.41, and c = 5.12	81.534	0.0023	66.24
10% AC	20.60	a = 4.67, b = 3.4, and c = 5.12	81.295	0.0023	60.56
15% AC	20.76	a = 4.66, b = 3.4, and c = 5.12	81.121	0.0023	49.51
20% AC	21.19	a = 4.66, b = 3.4, and c = 5.12	81.121	0.0022	41.92
25% AC	21.96	a = 4.66, b = 3.4, and c = 5.12	81.121	0.0021	39.84

composites in this study shows monoclinic phase for the copper oxide and similar for composites CuO–AC indicated the strong structural properties of CuO in composites [7, 30–32]. The main peaks clearly shows shifted to higher angle diffraction indicated decrease the lattice parameter and the volume in unit cell [1, 2, 32, 33]. Table 2 shows average crystal, dislocation density, lattice parameter, volume, and porosity of composite CuO–AC from the quantitative analysis of XRD spectra.

The average crystallite size (B) was calculated from the diffraction peaks using the Debye–Scherrer equations [1, 2],

$$D = \frac{K\lambda}{\beta \cos\theta} \tag{1}$$

where D is the crystallite size, k the shape factor, λ the wavelength of x-ray radiation, β is the full-width at half-maximum value of the diffraction angle θ. The dislocation density (δ) calculated by the following equation:

$$\delta = \frac{1}{D^2} \tag{2}$$

which are in agreement with some published works [1, 2, 13]. The lattice parameter for monoclinic structure $a \neq b \neq c$ was determined from the equation:

$$\frac{1}{d^2} = \frac{1}{\sin^2\beta}\left[\frac{h^2}{a^2} + \frac{k^2\sin^2\beta}{b^2} + \frac{l^2}{c^2} - \frac{2hl\cos\beta}{ac}\right] \tag{3}$$

The x-ray density (ρ_s), the experimental density (ρ_{ex}), and the porosity (P) of CuO and composite CuO–AC determined by using formula, respectively:

$$\rho_s = \frac{nM}{Nabc} = \frac{nM}{NV_{cal}} \tag{4}$$

$$\rho_{ex} = \frac{m}{V_{\exp}} \tag{5}$$

$$P = \left(1 - \frac{\rho_{ex}}{\rho_s}\right) \times 100\% \tag{6}$$

Where, n is the number of molecules per unit cell, for composites were the weighted average values for the number of molecules per unit cell of CuO and carbon. M is molecular weight, N is Avogadro number, a, b, and c is the lattice parameter from analysis of XRD spectra, and V_{cal} is the volume of the unit cell calculated from the lattice parameter. From the sample pellet preparation of XRD instrument, we determined the mass (m) and the volume (V_{exp}).

The lattice parameter for 10% AC shows the same with CuO as we expected and for >10% small decrease from CuO value but shows same lattice parameters even though the amount of AC increase up to 25% in composites. For porosity of composites shows decrease with increasing the amount of AC in composite, this probably due to the effectively pore of AC as organic linker in stabilizing the bonding formation, which may change the natural electronics and structural properties of composite CuO–AC. The strong bonding formation resulting in disorganization of the interaction between carbonaceous particle and CuO particles which may play an important role in the increasing magnetic and reflection loss properties.

Figure 4 shows the magnetic properties (a) and reflection loss (b) of CuO–AC bio-metal composite materials. The hysteresis loops of the composites, Coercivity and saturation magnetization values were investigated with an applied field of -10 kOe $< H <$ 10 kOe at room temperature using a vibrating sample magnetometer. The coercivity and the saturation magnetization of composite CuO–AC materials increase drastically with the increasing the amount of the AC particles in the composite as can be seen in table 3 for 15% AC and 25% AC. The saturation magnetization value for AC is 0.44 emu gr^{-1} higher than that of pure CuO is 0.0554 emu gr^{-1}. The bonding formation for composites CuO–AC in this study similar character composites as reported in [7] which can be controlled by the maximizing the functional of the pore and the amount of AC as an organic linker which exhibits in increased magnetic properties and enhanced absorption (reflection loss). For composites CuO–AC can be used in many other different field applications due to the stable bonding character.

Figure 4(b) shows the maximum reflection loss reaches 22.00 dB at 5.34 reflection loss of the composite for sample thickness 4 mm, for more details see table 4. For the reflection loss at -10 dB corresponds to the bandwidth frequency which was in the range of 1.29 to 2.19 GHz [29]. Stable bonding character and the amount of AC in the composites CuO–AC could effectively improve the electromagnetic waves absorbing properties at the frequency range of 5.2 GHz–5.86 GHz. Table 2 shows also the absorption properties as a function of the thickness of composites CuO–AC in this study. The bio-metal composites CuO–AC in this study is very promising EM wave absorber materials due the reflection loss (R) values less than -10 dB which can be designed to attenuate EM wave [7, 29]. For the reflection loss less than -10 dB is attributed to the dielectric loss

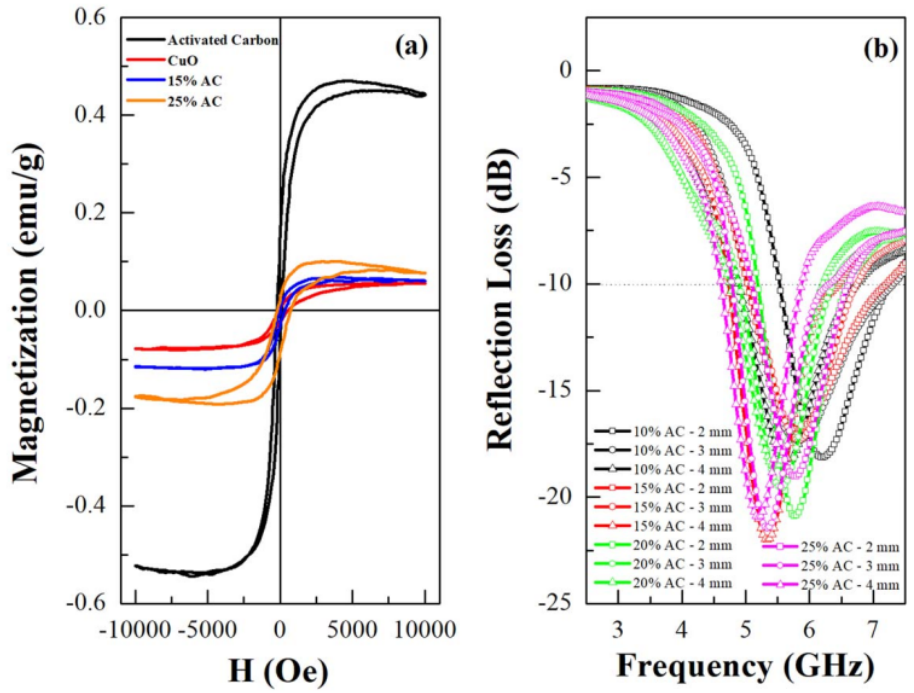

Figure 4. (a). Magnetic properties for AC, CuO and composite CuO–AC (15% and 25% AC). (b) Reflection loss properties for composite CuO–AC (10%, 15%, 20%, and 25% AC).

Table 3. Magnetic properties (H_c is coecivity, M_R is magnetic remanent, M_s is magnetic saturation) determined from figure 4(a) for AC, CuO, and composite CuO–AC (activated carbon) (15% AC and 25% AC).

Samples	H_C (±0.05 Oe)	M_R(±0.05 emu g^{-1})	M_S(±0.05 emu g^{-1})
AC	225.84	0.11	0.44
CuO	5.7182	0.000 66	0.0554
15% AC	11.4364	0.000 89	0.0607
25% AC	200.1372	0.018 56	0.0769

Table 4. Reflection Loss (RL) properties for composite CuO–AC (activated carbon) (10% AC, 15% AC, 20% AC, and 25% AC) determined from the figure 4(b).

Sample	Thickness (mm)	RL (dB)	Frequency (Hz)	Bandwidth
AC 10%	2	−18.13	6.18	1.67
	3	−17.36	5.86	2.19
	4	−18.44	5.66	1.75
AC 15%	2	−18.80	5.86	1.95
	3	−17.32	5.83	1.49
	4	−22.00	5.34	1.41
AC 20%	2	−20.88	5.76	1.29
	3	−19.56	5.55	1.33
	4	−18.54	5.48	1.32
AC 25%	2	−19.02	5.76	1.36
	3	−21.45	5.34	1.30
	4	−20.95	5.20	1.18

which was significantly higher than the magnetic losses [7, 33, 34]. In this present study shows the pore of AC effectively in modification electronic structure properties of composites which can be used to increase the stability bonding formation of CuO–AC material leading to increase the absorption (reflection loss) and magnetic properties.

4. Conclusions

We investigated the electronic properties by using XPS, REELS, and FTIR, the structural properties by XRD, and magnetic properties by VSM of CuO, AC and composite CuO–AC. These results showed that the composite CuO–AC have the mixed metal oxide and carbonaceous particles which indicated the modification of electronic structures of composite as O–C_x–$Cu_{1-x}O$ binary was formed. The core level spectra of Cu 2p, C1s, O 1s and full spectra as well as the band gaps of composite CuO–AC, CuO and AC which are in good agreement with previous results. It is found that the pore of AC effectively increase the stable bonding formation of composites CuO–AC material which leading to increase the absorption (reflection loss) and magnetic properties in devices applications.

Acknowledgments

This work was supported by the PBK (Penelitian Berbasis Kompetensi) Grant: 1625/UN4.21/PL.00.00/2018 funded by the Indonesian Government (Ristek-Dikti) and KLN Grant: 3083/UN4.1.2/PL.00.00/2018 funded by Hasanuddin University, Makassar Indonesia.

ORCID iDs

Dahlang Tahir https://orcid.org/0000-0002-8241-3604

References

[1] Chand P, Manisha M and Kumar P 2018 Effect of precursors medium on structural, optical and dielectric properties of CuO nastructures *Optik* **156** 743–53
[2] Svintsitskiy D A, Kardash T Y, Stonkus O A, Slavinskaya E M, Stadnichenko A I, Koscheev S V, Chupakhin A P and Boronin A I 2013 *In situ* XRD, XPS, TEM, and TPR study of highly active in CO oxidation CuO nanopowder *J. Phys. Chem.* C **117** 14588–99
[3] Oruc C and Altundal A 2017 Structural and dielectric properties of CuO nanoparticles *Ceram. Int.* **43** 10708–14
[4] De Souza V S, Da Frota H O and Sanches E A 2018 Polyaniline CuO hybrid nanocomposite with enhanced electrical conductivity *J. Mol. Struct.* **1153** 20–7
[5] Kuanr S K, Nayak S and Babu K S 2017 Ni dependent structural, optical and electrical properties of CuO nanostructures *Materials Science in Semiconductor Processing* **71** 268–74
[6] Ortiz R M, Garcia M M, Huerta J M M, Velarde J G C, Robles I E C and Guerrero A L 2018 Analysis of the magnetic properties in hard-magnetic nanofibers composite *J. Appl. Phys.* **123** 105108
[7] Tahir D, Ilyas S, Abdullah B, Armynah B and Kang H J 2018 Electronic properties of composite iron (II, III) oxide (Fe_3O_4) carbonaceous absorber materials by electron spectroscopy *J. Electron Spectrosc. Relat. Phenom.* **229** 47–51
[8] Kong I, Ahmad S H, Abdullah M H, Hui D, Yusoff A N and Puryanti D 2010 Magnetic and microwave absorbing properties of magnetite–thermoplastic natural rubber nanocomposites *J. Magn. Magn. Mater.* **322** 3401–9
[9] Shao L, Sang Y, Huang J and Liu Y N 2018 Triazine-based hyper-cross-linked polymers with inorganic-organic hybrid framework derived porous carbons for CO_2 capture *Chem. Eng. J.* **353** 1–14
[10] Praveen K T, Jay W G and Radha K M 2012 Facile xenon capture and release at room temperature using a metal–organic framework: a comparison with activated charcoal *Chem. Commun.* **48** 347–9
[11] Prasanth K P and Johnny D 2015 Doping activated carbon incorporated composite MIL-101 using lithium: impact on hydrogen uptake *J. Mater. Chem.* A **3** 7014–21
[12] Jang J S, Lee G W, Kim H, Hong S Y, Ci L, Nam J D and Suhr J 2018 High-damping and conducting epoxy nanocomposite using both zinc oxide particles and carbon nanofibers *Journal of Materiomics* **4** 187–93
[13] Hu X, Gao F, Xiang Y, Wu H, Zheng X, Jiang J, Li J, Yang H and Liu S 2016 Influence of oxygen pressure on the structural and electrical properties of CuO thin films prepared by pulsed laser deposition *Mater. Lett.* **176** 282–4
[14] Tahir D, Lee E K, Oh S K, Tham T T, Kang H J, Jin H, Heo S, Park J C, Chung J G and Lee J C 2009 Band alignment of atomic layer deposited $(ZrO_2)_x(SiO_2)_{1-x}$ gate dielectrics on Si (100) *Appl. Phys. Lett.* **94** 212902
[15] Tahir D, Lee E K, Oh S K, Kang H J, Heo S, Chung J G, Lee J C and Tougaard S 2009 Dielectrics and optical properties of Zr silicate thin films grown on Si (100) by atomic layer deposition *J. Appl. Phys.* **106** 084108
[16] Tahir D and Tougaard S 2012 Electronic and optical properties of selected polymers studied by reflection energy energy loss spectroscopy *J. Appl. Phys.* **111** 054101
[17] Tahir D and Tougaard S 2012 Electronic and optical properties of Cu, CuO and Cu_2O studied by electron spectroscopy *J. Phys. Condens. Matter* **24** 175002
[18] Romanyuk O, Jiricek P, Zemek J, Tougaard S and Paskova T 2011 Dielectric response function (0001), (1013) GaN single crystalline and disordered surface studied by reflection electron energy loss spectroscopy *J. Appl. Phys.* **110** 043507
[19] Denny Y S, Shin H C, Seo S, Oh S K, Kang H J, Tahir D, Heo S, Chung J G, Lee J C and Tougaard S 2012 Electronic and optical properties of hafnium indium zinc oxide thin film by XPS and REELS *J. Electron Spectrosc. Relat. Phenom.* **185** 18

[20] Heo S et al 2015 Band alignment of atomic layer deposited $(HfZrO_4)_{1-x}(SiO_2)$ gate dielectrics on Si (100) *Appl. Phys. Lett.* **107** 182101
[21] Shin H C, Tahir D, Seo S, Denny Y R, Oh S K, Kang H J, Heo S, Chung J G, Lee J C and Tougaard S 2012 Reflection electron energy loss spectroscopy for ultrathin gate oxide materials *Surf. Interface Anal.* **44** 623
[22] Tahir D, Kraaer J and Tougaard S 2014 Electronic and optical properties of Fe, Pd, and Ti studied by reflection electron energy loss spectroscopy *J. Appl. Phys.* **115** 243508
[23] Tahir D, Suarga, Sari N H and Yulianti Y 2015 Stopping powers and inelastic mean free path of 200 eV–50 keV electrons in polymer PMMA, PE, and PVC *Appl. Rad. Isotopes* **95** 59–62
[24] Tahir D, Lee E K, Choi E H, Oh S K, Kang H J, Heo S, Chung J G, Lee J C and Tougaard S 2010 Electronic and optical properties of Al_2O_3/SiO_2 thin films grown on Si substrate *J. Phys. D: Appl. Phys.* **43** 255301
[25] Tahir D, Cho Y J, Oh S K, Kang H J, Jin H, Heo S, Park J G, Lee J C and Tougaard S 2010 Electronic and optical properties of La-aluminate dielectric thin films on Si (100) *Surf. Interface Anal.* **42** 566–1569
[26] Tahir D, Lee E K, Oh S K, Kang H J, Lee E H, Chung J G, Lee J C and Tougaard S 2010 Electronic and optical properties of GIZO thin film grown on SiO2 substrate *Surf. Interface Anal.* **42** 906–10
[27] Tahir D, Oh S K, Kang H J and Tougaard S 2016 Quantitative analysis of reflection electron energy loss spectra to determine electronic and optical properties of Fe-Ni alloy thin films *J. Electron Spectrosc. Relat. Phenom.* **206** 6–18
[28] Tahir D, Oh S K, Kang H J and Tougaard S 2016 Composition dependence of dielectric and optical properties of Hf-Zr-silicate thin films grown on Si(100) by atomic layer deposition *Thin Solid Films* **616** 425–30
[29] Abdullah B, Ilyas S and Tahir D 2018 Nanocomposites Fe/activated carbon/PVA for microwave absorber: synthesis and characterization *Journal of Nanomaterials* **2018** Article ID 9823263 6
[30] Saini P, Singh M, Singh S P and Mahapatro A K 2018 Spectroscopic and electronic properties of polyallylamine functionalized graphene oxide films *Vacuum* **54** 110–4
[31] Costa P, Pereira J N, Oliveira J, Silva J, Moreira J A, Carabineiro S A C, Buijnsters J G and Mendez S L 2017 High-performance grapheme-based carbon nanofiller/polymer composites for piezoresistive sensor applications *Compos. Sci. Technol.* **153** 241–52
[32] Jensen B D, Odegard G M, Kim J W, Sauti G, Siochi E J and Wise K E 2018 Simulating the effects of carbon nanotube continuity and interfacial bonding on composite strength and stiffness *Compos. Sci. Technol.* **166** 10–9
[33] Liu X, Xu F, Zhang K, Wei B, Gao Z and Qiu Y 2017 Characterization of enhanced interfacial bonding between epoxy and plasma functionalized carbon nanotube films *Compos. Sci. Technol.* **145** 114–21
[34] Yu H, Xin G, Ge X, Bulin C, Li R, Xing R and Zhang B 2018 Porous graphene-polyaniline nanoarrays composite with enhanced interface bonding and electrochemical performance *Composite Science and Technology* **154** 76–84

Tahir_2019_Mater._Res._Express_6_035705.pdf

ORIGINALITY REPORT

18%	%	18%	%
SIMILARITY INDEX	INTERNET SOURCES	PUBLICATIONS	STUDENT PAPERS

PRIMARY SOURCES

1	Deepak Sharma, Prakriti Kumar Ghosh, Ramkishor Anant, Sudhir Kumar. "Surface modification of microalloyed steel by silicon carbide reinforcement using tungsten inert gas arcing", Materials Research Express, 2018 Publication	2%
2	Heryanto Heryanto, Dahlang Tahir. " High Absorption Electromagnetic Wave Properties of Composite CoFeO Synthesized by Simple Mechanical Alloying ", ECS Journal of Solid State Science and Technology, 2021 Publication	1%
3	Bualkar Abdullah, An Nisyah, Sultan Ilyas, Dahlang Tahir. " Structural properties and bonding characteristics of honeycomb structure of composite ZnMnO and activated carbon ", Journal of Applied Biomaterials & Functional Materials, 2019 Publication	1%
4	Dahlang Tahir, Ruzaini H. Abidin, Paulus Lobo Gareso. " High Efficiency Dye Sensitized Solar	1%

Cell from and red as a Sensitizer ", IOP Conference Series: Earth and Environmental Science, 2019
Publication

---

5 Dahlang Tahir. "Electronic and optical properties of La-aluminate dielectric thin films on Si (100)", Surface and Interface Analysis, 07/20/2010 — 1 %
Publication

---

6 Roni Rahmat, Heryanto Heryanto, Sultan Ilyas, Ahmad Nurul Fahri, Inayatul Mutmainna, Mufti Hatur Rahmi, Dahlang Tahir. "The relation between structural, optical, and electronic properties of composite CuO/ZnO in supporting photocatalytic performance", DESALINATION AND WATER TREATMENT, 2022 — 1 %
Publication

---

7 Dahlang Tahir, Eun Kyoung Lee, Suhk Kun Oh, Tran Thi Tham et al. "Band alignment of atomic layer deposited (ZrO2)x(SiO2)1−x gate dielectrics on Si (100)", Applied Physics Letters, 2009 — 1 %
Publication

---

8 Hendri, B Abdullah, D Tahir, S Fatimah. "New types composite copper (Cu) and activated carbon (C) for electromagnetic wave absorber — 1 %

materials", Journal of Physics: Conference Series, 2019
Publication

9	Ahmad, Shabir, Mohd. Nasir, K. Asokan, Mohd. Shahid Khan, and M. Zulfequar. "Electronic excitation induced structural, optical and electrical properties of Se85S10Zn5 thin films and applicability of a single oscillator model", RSC Advances, 2015. Publication	1 %
10	Dahlang Tahir, Suhk Kun Oh, Hee Jae Kang, Sven Tougaard. "Composition dependence of dielectric and optical properties of Hf-Zr-silicate thin films grown on Si(100) by atomic layer deposition", Thin Solid Films, 2016 Publication	1 %
11	Sung Heo, Dahlang Tahir, Jae Gwan Chung, Jae Cheol Lee et al. " Band alignment of atomic layer deposited (HfZrO) (SiO) gate dielectrics on Si (100) ", Applied Physics Letters, 2015 Publication	<1 %
12	Dahlang Tahir, Jens Kraaer, Sven Tougaard. "Electronic and optical properties of Fe, Pd, and Ti studied by reflection electron energy loss spectroscopy", Journal of Applied Physics, 2014 Publication	<1 %

13	Hua Jin. "Band gap engineering for La aluminate dielectrics on Si (100)", Applied Physics Letters, 2008 Publication	<1 %
14	Yus Rama Denny, Hye Chung Shin, Soonjoo Seo, Suhk Kun Oh et al. "Electronic and optical properties of hafnium indium zinc oxide thin film by XPS and REELS", Journal of Electron Spectroscopy and Related Phenomena, 2012 Publication	<1 %
15	H Trombini, M Vos, R G Elliman, P L Grande. "Depth profiling of ion-implanted samples by high-energy electron scattering", Journal of Physics D: Applied Physics, 2020 Publication	<1 %
16	Juan Ding, Ying Huang, Tiaozheng Han, Yanli Wang. "Synthesis of functionalized graphene oxide nanoflakes using silane coupling agents", High Performance Polymers, 2015 Publication	<1 %
17	M. Nirouei, A. Jafari, K. Boustani. "Magnetic and Structural Study of FeNi3 Nanoparticles: Effect of Calcination Temperature", Journal of Superconductivity and Novel Magnetism, 2014 Publication	<1 %

18	L H Yang, K Tőkési, J Tóth, B Da, Z J Ding. "Revision of optical property of silicon by a reverse Monte Carlo analysis of reflection electron energy loss spectroscopy spectra", Journal of Physics: Conference Series, 2020 Publication	<1 %
19	R. Murillo-Ortíz, M. Mirabal-García, J. M. Martínez-Huerta, J. G. Cabal Velarde, I. E. Castaneda-Robles, A. Lobo-Guerrero. "Analysis of the magnetic properties in hard-magnetic nanofibers composite", Journal of Applied Physics, 2018 Publication	<1 %
20	B.K. Money, K. Hariharan. "Lithium ion conduction in lithium metaphosphate based systems", Applied Physics A, 2007 Publication	<1 %
21	Ardiansyah Ardiansyah, Roni Rahmat, Muhammad Azlan, Heryanto Heryanto, Dahlang Tahir. "Nanocrystal composites cement/BaCO3/Fe2O3 for improved X-ray shielding characteristics: Stability structural properties", Journal of Materials Research, 2022 Publication	<1 %
22	F. J. Boerio, P. Shah. "Adhesion of Injection Molded PVC to Steel Substrates", The Journal of Adhesion, 2005	<1 %

Publication

23	Ahmet Teber, Kadir Cil, Turgut Yilmaz, Busra Eraslan, Dilara Uysal, Gokce Surucu, Abdul Baykal, Rajeev Bansal. "Manganese and Zinc Spinel Ferrites Blended with Multi-Walled Carbon Nanotubes as Microwave Absorbing Materials", Aerospace, 2017 Publication	<1 %
24	Butcher, K.. "Gallium and oxygen accumulations on gallium nitride surfaces following argon ion milling in ultra-high vacuum conditions", Applied Surface Science, 20040531 Publication	<1 %
25	J. H. Jeon, Y. H. Hwang, B. S. Bae, H. L. Kwon, H. J. Kang. "Addition of aluminum to solution processed conductive indium tin oxide thin film for an oxide thin film transistor", Applied Physics Letters, 2010 Publication	<1 %
26	Kristina M. Herman, Sotiris S. Xantheas. "A Formulation of the Many-Body Expansion (MBE) for Periodic Systems: Application to Several Ice Phases", The Journal of Physical Chemistry Letters, 2023 Publication	<1 %
27	Sung Heo, Hyung-Ik Lee, Taewon Song, Jong-Bong Park et al. " Direct band gap	<1 %

measurement of Cu(In,Ga)(Se,S) thin films using high-resolution reflection electron energy loss spectroscopy ", Applied Physics Letters, 2015
Publication

---

28 Ahmed S. Jbara, Zulkafli Othaman, M.A. Saeed. "Structural, morphological and optical investigations of θ-Al 2 O 3 ultrafine powder", Journal of Alloys and Compounds, 2017 <1%
Publication

---

29 Bidayatul Armynah, Dahlang Tahir, Monalisa Tandilayuk, Zuryati Djafar, Wahyu H. Piarah. "Potentials of Biochars Derived from Bamboo Leaf Biomass as Energy Sources: Effect of Temperature and Time of Heating", International Journal of Biomaterials, 2019 <1%
Publication

---

30 I Mutmainna, D Tahir, P L Gareso, S Ilyas, A Saludung. "Improving Degradation Ability of Composite Starch/Chitosan by Additional Pineapple Leaf Microfibers for Food Packaging Applications", IOP Conference Series: Materials Science and Engineering, 2019 <1%
Publication

---

31 Zhenjie Tang, Rong Li, Xiwei Zhang, Huijuan Geng, Shuaipu Zang, Huiyuan Zheng, Mengchen Lian, Niannian Hu. "Correlation <1%

between memory characteristics and energy band bending resulted from composition distribution of trapping layer for charge trap memory", Semiconductor Science and Technology, 2018
Publication

---

32 Dahlang Tahir. "Band alignment of atomic layer deposited (ZrO[sub 2])[sub x](SiO[sub 2])[sub 1−x] gate dielectrics on Si (100)", Applied Physics Letters, 2009 <1 %
Publication

---

33 Degang Deng, Hua Yu, Yinqun Li, Youjie Hua et al. "Ca4(PO4)2O:Eu2+ red-emitting phosphor for solid-state lighting: structure, luminescent properties and white light emitting diode application", Journal of Materials Chemistry C, 2013 <1 %
Publication

---

34 Hadis Morkoç, Ümit Özgür. "Zinc Oxide", Wiley, 2009 <1 %
Publication

---

35 Hyeonchul Lee, Minsu Jeong, Gahui Kim, Kirak Son, Jeongmin Seo, Taek-Soo Kim, Young-Bae Park. "Effects of Post-annealing and Co Interlayer Between SiNx and Cu on the Interfacial Adhesion Energy for Advanced Cu Interconnections", Electronic Materials Letters, 2020 <1 %
Publication

36	J M Michalik. "Temperature dependence of magnetization under high fields in Re-based double perovskites", Journal of Physics Condensed Matter, 12/19/2007 Publication	<1 %
37	P. Costa, J. Nunes-Pereira, J. Oliveira, J. Silva et al. "High-performance graphene-based carbon nanofiller/polymer composites for piezoresistive sensor applications", Composites Science and Technology, 2017 Publication	<1 %
38	Siti Fatimah, Silma Maula Bilqis, Isnaeni, Dahlang Tahir. "Luminescence properties of carbon dots synthesis from sugar for enhancing glows in paints", Materials Research Express, 2019 Publication	<1 %
39	Sri Suryani, Asni Damayanti, Heryanto Heryanto, Roni Rahmat, Syarifuddin Syarifuddin, Dahlang Tahir. "High efficiency self-cleaning of nanocomposites ZnO with additional chitosan for helping electron and hole transport", International Journal of Biological Macromolecules, 2022 Publication	<1 %
40	Sung Heo, JaeGwan Chung, Jae Cheol Lee, Taewon Song et al. " Band alignment and defect states in amorphous GaInZnO thin	<1 %

films grown on SiO /Si substrates ", Surface and Interface Analysis, 2016
Publication

---

41 Yongqing Li, Qun Wang. "Composition control and selective infrared radiative properties of copper alloy oxides by DC reactive sputtering", Journal of Physics: Conference Series, 2022 <1 %
Publication

---

42 Hua Jin. "Electronic properties of ultrathin (HfO[sub 2])[sub x](SiO[sub 2])[sub 1−x] dielectrics on Si (100)", Journal of Applied Physics, 2007 <1 %
Publication

---

43 Soumyaditya Sutradhar, Suman Saha, Sana Javed. "Shielding Effectiveness Study of Barium Hexaferrite-Incorporated, β-Phase-Improved Poly(vinylidene fluoride) Composite Film: A Metamaterial Useful for the Reduction of Electromagnetic Pollution", ACS Applied Materials & Interfaces, 2019 <1 %
Publication

---

44 Xiaoli Wei, Yinghan He, Kaiyang Liu, Pengxiang Gao, Xiuli Chen, Xiaobin Liu, Huanfu Zhou. "Sintering behavior, crystal structure, and microwave dielectric properties of a novel diopside SrMgGe2O6 ceramic and adjustment of its τf value", Ceramics International, 2022 <1 %
Publication

45	Elsayed Elgazzar, Ragab A.M. Said, Adham A. El-Zomrawy, Ashraf M. Ashmawy et al. "The fabrication of an innovative extremely sensitive nano green carbon paste electrode amended with the nanocomposite CuO/Y for electrochemical quantification of amprolium in sheep meat and liver samples", Food Chemistry, 2022 Publication	<1 %
46	S. Tanuma, C. J. Powell, D. R. Penn. "Calculations of electron inelastic mean free paths. V. Data for 14 organic compounds over the 50-2000 eV range", Surface and Interface Analysis, 1994 Publication	<1 %

Exclude quotes	On	Exclude matches	< 4 words
Exclude bibliography	On		